

April 01, 2003

Magnetic and microwave magnetic properties of barium hexaferrite permanent magnet films having the c-axis in the film plane

S. D. Yoon

C. Vittoria
Northeastern University

S. A. Oliver

Recommended Citation

Yoon, S. D.; Vittoria, C.; and Oliver, S. A., "Magnetic and microwave magnetic properties of barium hexaferrite permanent magnet films having the c-axis in the film plane" (2003). *Electrical and Computer Engineering Faculty Publications*. Paper 69.
<http://hdl.handle.net/2047/d20002240>



Magnetic and microwave magnetic properties of barium hexaferrite permanent magnet films having the c-axis in the film plane

S. D. Yoon, C. Vittoria, and S. A. Oliver

Citation: *J. Appl. Phys.* **93**, 4023 (2003); doi: 10.1063/1.1544083

View online: <http://dx.doi.org/10.1063/1.1544083>

View Table of Contents: <http://jap.aip.org/resource/1/JAPIAU/v93/i7>

Published by the [American Institute of Physics](#).

Related Articles

Large anisotropic remnant magnetization tunability in (011)-La₂/3Sr₁/3MnO₃/0.7Pb(Mg₂/3Nb₁/3)O₃-0.3PbTiO₃ multiferroic epitaxial heterostructures
Appl. Phys. Lett. **100**, 043506 (2012)

Induced magnetic anisotropy and spin polarization in pulsed laser-deposited Co₂MnSb thin films
J. Appl. Phys. **111**, 023903 (2012)

Room temperature ferromagnetism in transparent Fe-doped In₂O₃ films
Appl. Phys. Lett. **100**, 032404 (2012)

Chemical ordering of FePt films using millisecond flash-lamp annealing
J. Appl. Phys. **111**, 023902 (2012)

Probing origin of room temperature ferromagnetism in Ni ion implanted ZnO films with x-ray absorption spectroscopy
J. Appl. Phys. **111**, 013715 (2012)

Additional information on *J. Appl. Phys.*

Journal Homepage: <http://jap.aip.org/>

Journal Information: http://jap.aip.org/about/about_the_journal

Top downloads: http://jap.aip.org/features/most_downloaded

Information for Authors: <http://jap.aip.org/authors>

ADVERTISEMENT

LakeShore Model 8404 developed with **TOYO Corporation**
NEW AC/DC Hall Effect System Measure mobilities down to 0.001 cm²/V s

Magnetic and microwave magnetic properties of barium hexaferrite permanent magnet films having the *c*-axis in the film plane

S. D. Yoon^{a)} and C. Vittoria

Department of Electrical and Computer Engineering, Northeastern University, Boston, Massachusetts 02115

S. A. Oliver

Center for Subsurface Sensing and Imaging Systems, Northeastern University, Boston, Massachusetts 02115

(Received 13 June 2002; accepted 14 December 2002)

Thick (1–14 μm) films of ferrimagnetic barium hexaferrite ($\text{BaFe}_{12}\text{O}_{19}$ or BaM) having the *c*-axis ([0001]) in the film plane were deposited by pulsed laser deposition onto *a*-plane (11 $\bar{2}$ 0) sapphire (Al_2O_3) substrates, and were found to have a (10 $\bar{1}$ 0) orientation. Torque and magnetization measurements show these films are permanent magnets with easy magnetization direction in the plane of the film. Ferrimagnetic resonance (FMR) spectra exhibited linewidths of 1.00–1.40 kOe, where low-field FMR measurements do not show uniform mode broadening due to the formation of multiple domains. All film parameters were affected by the large stress present in these films due to crystallographic and thermal mismatches. These films have dual functionality as gyrotropic media and permanent magnets, and are usable as either nonreciprocal microwave devices or biasing magnets. © 2003 American Institute of Physics. [DOI: 10.1063/1.1544083]

I. INTRODUCTION

Thick highly oriented films of hexagonal ferrites (hexaferrites) having uniaxial magnetocrystalline anisotropy are promising candidates for planar nonreciprocal devices operating at microwave and millimeter wavelengths. Although commonly used as permanent magnets, hexaferrites are not usually employed as microwave ferrites, in part due to the well-established usage of garnet and spinel ferrites, but also because ferrite materials are best employed at frequencies above 20 GHz that are only now becoming technologically important. The hexaferrite materials provide dual functionality, since they possess gyrotropic properties that allow for nonreciprocal microwave devices, and also provide magnetic self-biasing through the large uniaxial magnetocrystalline anisotropy that makes them valuable as permanent magnets. It is this dual functionality that allows one to apply hexaferrite materials in devices at frequencies that are inaccessible to traditional microwave ferrites.^{1,2}

The large uniaxial anisotropy present in barium hexaferrite ($\text{BaFe}_{12}\text{O}_{19}$) is coincident with the *c*-axis of the hexagonal unit cell, such that the easy axis of the magnetization lies along the [0001] direction. In general, different types of microwave devices have different operational requirements with respect to the orientation of the ferrite magnetization vector and the microwave propagation vector. Thus, it is important to grow and measure the properties of hexaferrite films where the easy axis of magnetization lies in the film plane, and also where the easy axis is normal to the film plane. However, the majority of research on hexaferrite films has focused on the latter case, i.e., the deposition of (0001) hexaferrite films. Such films have been deposited onto either (0001) sapphire (Al_2O_3) substrates^{3–7} or (111) magnesium

oxide substrates,⁸ and have been found to have good-to-excellent film epitaxy, magnetic properties, and microwave magnetic properties. However, these films do not yet show true dual functionality since the shape demagnetizing field in this film geometry overcomes the moderate coercive field present in these high-quality crystalline materials, such that they are partially demagnetized and suffer diminished microwave magnetic properties.

In contrast to work on (0001) hexaferrite films, this work considers thick highly oriented barium hexaferrite films that have the easy axis in the film plane. Although limited research has been done previously on such hexaferrite films,^{4,5,9} it has not been previously appreciated that crystalline hexaferrite films having in-plane anisotropy (*c*-axis in the film plane) behave as permanent magnets even when their coercive field is low, such that they provide dual functionality for truly self-biased planar microwave devices. In addition to their usefulness as self-biased microwave materials, these films may also be useful as a biasing magnet for nonmicrowave applications, especially for systems where a nonmetallic permanent magnet film is desirable.

II. EXPERIMENT

The $\text{BaFe}_{12}\text{O}_{19}$ films described here were deposited by pulsed laser ablation from 99.9% pure $\text{BaFe}_{12}\text{O}_{19}$ targets onto polished 1 cm \times 1 cm *a*-plane (11 $\bar{2}$ 0) sapphire substrates. The energy of the excimer laser (248 nm) beam was fixed at 500 mJ, and the beam was focused to obtain a laser fluence on the target of 4–5 J/cm², where the target was rotated and rastered so as to minimize the effects of target aging. Film depositions were done at a laser repetition rate of 50 Hz at an oxygen pressure of 20 mTorr. The substrate was

^{a)}Electronic mail: syoon@ece.neu.edu

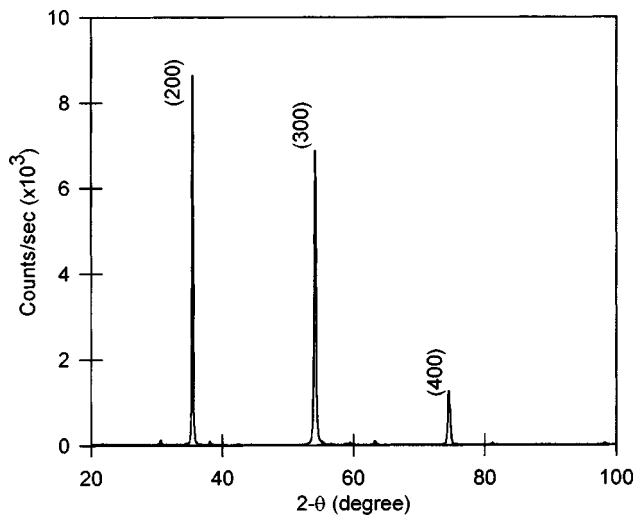


FIG. 1. $\text{Cu } K\alpha_1$ radiation source of x-ray diffraction pattern for a $7.0 \mu\text{m}$ $\text{BaFe}_{12}\text{O}_{19}$ film showing diffraction peaks from the $\text{BaFe}_{12}\text{O}_{19}$ (1010) planes.

heated both by resistive heating and by an *in situ* halogen lamp, with all quoted temperatures being that of the heater block. Thicker films deposited at temperatures of 900°C and above showed strong morphological instabilities, with the surface being covered with tall uniformly spaced spires. In contrast, films deposited at 840°C had few outgrowths. All of the as-produced films reported on here were deposited at 840°C and were grown to thickness of 1 to $14 \mu\text{m}$.

III. RESULTS AND DISCUSSION

$\text{Cu } K\alpha_1$ radiation source of x-ray diffraction measurements showed that these films have an in-plane (1010) orientation, as shown in the diffraction pattern for a $7.0 \mu\text{m}$ $\text{BaFe}_{12}\text{O}_{19}$ film shown in Fig. 1. This correspondence between the $\text{BaFe}_{12}\text{O}_{19}$ (1010) and sapphire (1120) orientations has been noted previously for $\text{BaFe}_{12}\text{O}_{19}$ films on both *c*-plane and *a*-plane sapphire substrates.⁹ In addition, the [0001] axes of both the film and substrate are collinear. A lattice constant of $a = 5.887 \text{ \AA}$ was found for this film by fitting the centroids of the (2020), (3030), and (4040) reflection peaks to the Bragg diffraction law, in good agreement with literature values.^{10,11} A rocking curve taken around the (2020) diffraction peak for this sample yielded a broad symmetric peak having a full width half maximum value of 1.88° , indicating that substantial lattice dispersion exists in this film.

Stress effects are clearly present in thicker films, and may cause the substantial lattice dispersion. Films thicker than $\sim 5 \mu\text{m}$ show regions where the films fractured in long parallel strips spaced a few tens of micrometers apart. Strip delamination occurred, see Fig. 2, for portions of the thickest films ($> 10 \mu\text{m}$), where the fracture always occurred in the sapphire substrate. When referenced to the in-plane magnetization axes, the long axis of these strips closely correspond to the in-plane hard axis, so the easy axis of magnetization lay transverse to the cracks. This stress and fracturing arises from mismatches in crystal structure, lattice constants, and thermal coefficients of expansion between $\text{BaFe}_{12}\text{O}_{19}$ and

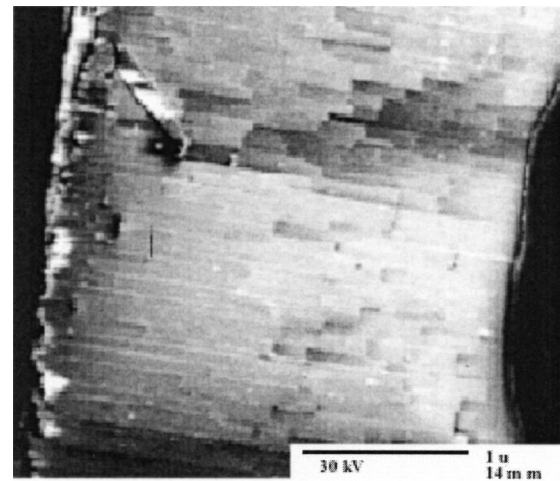


FIG. 2. Scanning electron microscopy morphology for $7.0 \mu\text{m}$ $\text{BaFe}_{12}\text{O}_{19}$ film.

sapphire. In particular, the *a*-lattice and *c*-lattice constants are $a = 4.7588 \text{ \AA}$ and $c = 12.992 \text{ \AA}$ for sapphire,¹² and $a = 5.89 \text{ \AA}$ and $c = 23.2 \text{ \AA}$ ^{10,11} for $\text{BaFe}_{12}\text{O}_{19}$. Of more importance for these thick films, the coefficients of thermal expansion for barium hexaferrite^{10,11} and Al_2O_3 (Ref. 13) are anisotropic and temperature dependent, such that the thermally induced stress is anisotropic in the film plane. Here, the observed fracture and delamination patterns indicate that the $\text{BaFe}_{12}\text{O}_{19}$ film [0001] direction is under tensile stress, while the $\text{BaFe}_{12}\text{O}_{19}$ [1010] axis experiences a smaller, possibly compressive, stress.

The magnetic properties of $\text{BaFe}_{12}\text{O}_{19}$ films having in-plane uniaxial anisotropy axis are typified by the hysteresis loops shown in Fig. 3 and the in-plane torque magnetometer results of Fig. 4. Figure 3 shows three hysteresis loops corresponding to the applied magnetic field (*H*) being applied along the in-plane easy and hard axes, and the film normal, which is also a hard axis. Both hard axis loops have small coercive field values ($H_c < 100 \text{ Oe}$) and vary somewhat from

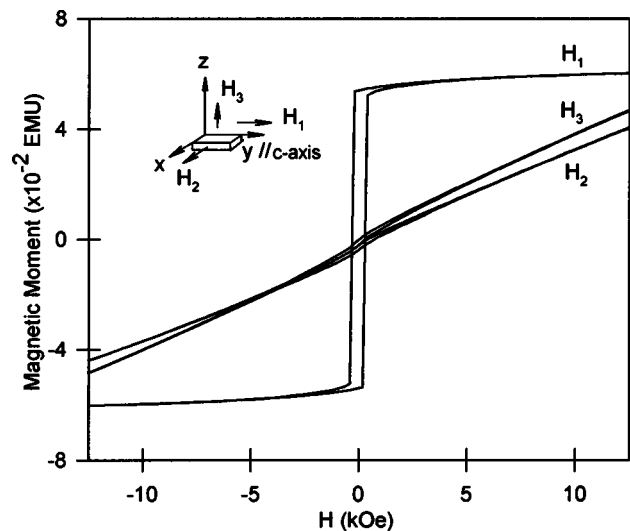


FIG. 3. Hysteresis loops for a $7.0 \mu\text{m}$ $\text{BaFe}_{12}\text{O}_{19}$ film with *H* along the easy axis, in-plane hard axis, and film normal.

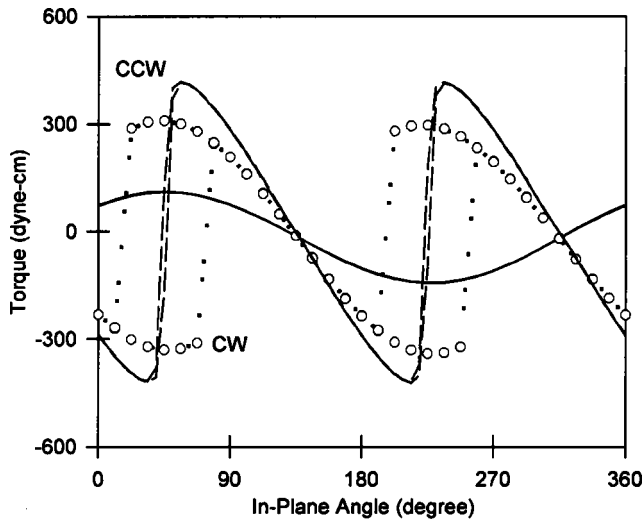


FIG. 4. In-plane torque loops are shown for a 7.0 μm $\text{BaFe}_{12}\text{O}_{19}$ film for three applied fields: $H=200$ Oe (solid line— $\times 20$) showing magnetic dipole behavior, and $H=500$ Oe (dotted lines— $\times 10$), and $H=10$ kOe (dashed line) showing uniaxial anisotropy behavior.

a linear behavior. The deviation from linearity at low fields may be due to a number of effects: (1) some ferrite was deposited along the edge of the substrate, and (2) inclusion of nonuniformities within the sample as evidenced by the cracks. Neither loop could be saturated due to insufficient magnetic field, and the lower slope of the out-of-plane hard axis arises from the requirement that the saturating field must overcome both the shape demagnetizing field ($4\pi M_s$) and the uniaxial anisotropy field (H_A) along the film normal. Other films show hard axis coercive field values of under 30 Oe. Easy axis hysteresis loops show good square loop behavior with loop squareness values of 0.93–0.95 and $H_c=250-450$ Oe, as is typified in Fig. 2. Initial magnetization measurements on dc demagnetized samples show that H_c can be solely attributed to domain-wall pinning. Values for the saturation magnetization ($4\pi M_s=4.0\pm 0.2$ kG) and $H_A=15.9\pm 0.3$ kOe were obtained from magnetization and torque results, and are in good agreement with those from other barium hexaferrite films,^{4,7,8} although these results are consistently below bulk values.¹⁴

The relatively small coercive field value of each film yields a small energy product. However, these small coercive fields are sufficiently large to permanently magnetize the films since the shape-demagnetizing factor in the film plane approaches zero. This is illustrated by the in-plane torque measurements of Fig. 3, which were taken on a disk-shaped sample at applied fields of 200 Oe, 500 Oe, and 10 kOe where the plane of the disk was rotated both clockwise (CW) and counter-clockwise (CCW) in the applied field. Here the torque results for the $H=200$ Oe ($H=500$ Oe) measurements have been scaled by $\times 20$ ($\times 10$) to allow for a shape comparison with the 10 kOe results. Note that the torque curves taken at $H=200$ Oe show only the sinusoidal dependence typical of a magnetic dipole, as expected for a permanent magnet. Meanwhile, the torque measurements at higher fields ($H>H_c$) shows the behavior expected for a film having a large in-plane uniaxial anisotropy axis, since the mag-

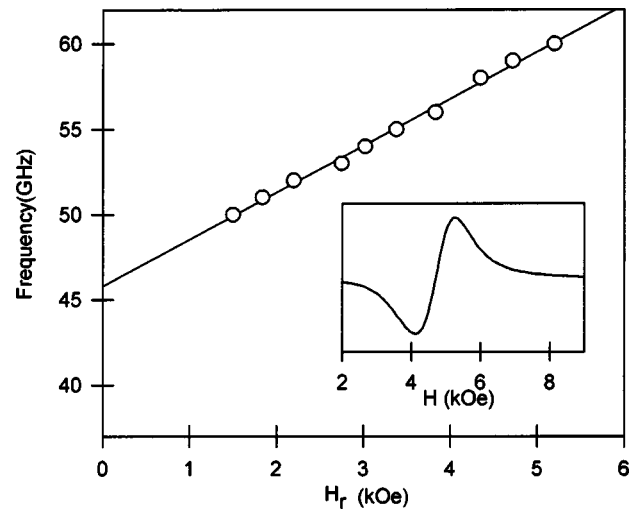


FIG. 5. Frequency vs FMR resonant field behavior of a 7.0 μm $\text{BaFe}_{12}\text{O}_{19}$ film. The solid line is a fit to the data. Inset: FMR spectrum for $f=59$ GHz.

netization vector is no longer pinned. Here, the abrupt breaks seen in the CW and CCW torque curves correspond to magnetization jumps across the hard axis.

Ferrimagnetic resonance spectra were taken with H placed along the film easy axis using a standard differential power absorption technique where the film was mounted in a shorted transverse electric (TE_{10}) waveguide. The ferrimagnetic resonance (FMR) condition can be evaluated from the magnetic free energy in a single domain film, and is given by

$$F(\text{ergs}/\text{cm}^3) = -M \cdot H^p + 2\pi M_s^2 \sin^2 \theta \cos^2 \phi - K_1 \sin^2 \theta \cos^2 \phi, \quad (1)$$

where K_1 is the first-order magnetocrystalline anisotropy constant, and the magnetization angles $M(\theta, \phi)$ are defined with respect to the film normal and in-plane easy axis, respectively. These three free energy terms encompass the Zeeman magnetizing energy, the shape demagnetizing energy, uniaxial anisotropy magnetic energy, respectively. We have chosen the easy axis of magnetization along the x axis in the film plane. The resulting ferrimagnetic resonance (FMR) condition when \mathbf{H} and \mathbf{M} lie along the film easy axis ($\theta = \pi/2$ and $\phi = 0$) is then

$$\frac{\omega}{\gamma} = \sqrt{(H_r + H_A + 4\pi M_s)(H_r + H_A)}, \quad (2)$$

where H_r is the resonant magnetic field obtained for a microwave frequency $f = \omega/2\pi$, $H_A = 2K_1/M_s$, and γ is the gyromagnetic ratio. Most FMR spectrum measured in the frequency range from 51 to 61 GHz showed Lorentzian absorptions, and an FMR spectra obtained at 59 GHz for the 7.0 μm film is shown in the inset of Fig. 5. In addition, Fig. 5 shows a plot of microwave frequency versus resonant field for the same film, where the solid line shows the best fit of Eq. (2) to the data, where the fit parameters were $\gamma/2\pi = 2.72 \pm 0.06$ GHz/kOe, $H_A = 15.1 \pm 0.2$ kOe, and $4\pi M_s = 3.8 \pm 0.2$ kG.

Two important results were obtained from such microwave magnetic measurements. First, the intercept of the frequency resonance versus resonant field at 46 GHz yields the self-resonance frequency of the film, which governs the operational frequency of prospective millimeter wavelength devices. More significantly, the FMR linewidths (ΔH) of these samples remain constant throughout the frequency range measured, which for the film of Fig. 4 yields an averaged linewidth of $\Delta H = 1.15 \pm 0.01$ kOe from all points. Thus, the magnetic loss parameter for these films, as given by the FMR linewidth, does not experience the detrimental effects incurred by the formation of multiple domains when ferrites become partially demagnetized, as for example occurs in (0001) BaFe₁₂O₁₉ films^{4,8} when $H < 4\pi M_s$. This important property is a direct result of the permanent magnet properties of these films, and is a key factor in the utility of these films for microwave devices.

The FMR linewidth values obtained for these (1010) films are twice those measured for (0001) BaFe₁₂O₁₉ films of similar thickness grown under similar deposition conditions,⁷ and are far from the intrinsic FMR linewidth value of $\Delta H \approx 10-30$ Oe.^{14,15} One macroscopic source for linewidth broadening arises from the dispersion in the orientation of the anisotropy easy axis from grain to grain within a mosaic structure, such that the FMR condition differs between grains. Such a dispersion in grain orientation can be inferred from the broad x-ray diffraction rocking curve and the 5% variation in easy axis hysteresis loop squareness from one. Two-magnon scattering processes may also contribute to broadening of the uniform mode. Source of two-magnon processes could be due to scattering from magnetic defects, voids, compositions, and crystal irregularities. Magnetic irregularities can be at the surface or in the volume of the sample. The fact that H_c is rather small, we attribute the linewidth broadening to surface roughness and cracking of the samples.¹⁶ In order to reduce the magnetic losses in these

permanent magnet films, it will be necessary to understand and reduce the linewidth of the uniform FMR mode, which in turn may be intimately connected to controlling the film growth and stress mechanisms within the BaFe₁₂O₁₉/sapphire (Al₂O₃) system.

ACKNOWLEDGMENT

This work was supported in part by the United States Office of Naval Research and Defense Advanced Research Projects Agency under the 1996 Multidisciplinary University Research Initiative.

- ¹Y. Akaiwa and T. Okazaki, *IEEE Trans. Magn.* **10**, 374 (1974).
- ²S. A. Oliver, P. Shi, W. Hu, H. How, S. W. McKnight, N. E. McGruer, P. M. Zavracky, and C. Vittoria, *IEEE Trans. Microwave Theory Tech.* **49**, 385 (2001).
- ³C. A. Carosella, D. B. Chrisey, P. Lubitz, J. S. Horwitz, P. Dorsey, R. Seed, and C. Vittoria, *J. Appl. Phys.* **71**, 5107 (1992).
- ⁴P. C. Dorsey, D. B. Chrisey, J. S. Horwitz, P. Lubitz, and R. C. Y. Auy-eung, *IEEE Trans. Magn.* **30**, 4512 (1994).
- ⁵T. L. Hylton, M. A. Parker, K. R. Coffey, and J. K. Howard, *J. Appl. Phys.* **73**, 6257 (1993).
- ⁶S. R. Shinde, R. Ramesh, S. E. Lofland, S. M. Bhagat, S. B. Ogale, R. P. Sharma, and T. Venkatesan, *Appl. Phys. Lett.* **72**, 3443 (1998).
- ⁷S. A. Oliver, M. L. Chen, L. Kozulin, and C. Vittoria, *J. Magn. Magn. Mater.* **213**, 326 (2000).
- ⁸S. A. Oliver, S. D. Yoon, I. Kozulin, M. L. Chen, and C. Vittoria, *Appl. Phys. Lett.* **76**, 3612 (2000).
- ⁹T. L. Hylton, M. A. Parker, and J. K. Howard, *Appl. Phys. Lett.* **61**, 867 (1992).
- ¹⁰P. C. Dorsey, S. B. Qadri, J. L. Feldman, J. S. Horwitz, P. Lubitz, D. B. Chrisey, and J. B. Ings, *J. Appl. Phys.* **79**, 3517 (1996).
- ¹¹D. Sriram, R. L. Snyder, and V. R. W. Amarakoon, *J. Mater. Res.* **15**, 1349 (2000).
- ¹²International Centre for Diffraction Data (ICDD) card number 42-1468.
- ¹³*CRC Materials Science and Engineering Handbook* (CRC, Boca Raton, 1994), pp. 308-309.
- ¹⁴H. Kojima, in *Ferromagnetic Materials*, edited by E. P. Wohlfarth (North-Holland, Amsterdam, 1982), vol. 3, p. 305.
- ¹⁵S. G. Wang, S. D. Yoon, and C. Vittoria, *J. Appl. Phys.* **92**, 6728 (2002).
- ¹⁶A. M. Clogston, H. Suhl, L. R. Walker, and P. W. Anderson, *J. Phys. Chem. Solids* **1**, 129 (1956).